Signals of quark-hadron phase transition in neutron star mergers

Martin Urbanec

Silesian University in Opava

AI&GW@CZ, Prague   28/11/2025

Neutron stars

- Compact objects – radius around 10km for 1.4 MSUN (1.5 – 4. times the radius of a BH)
- Density in the cores 3-5 x nuclear matter density

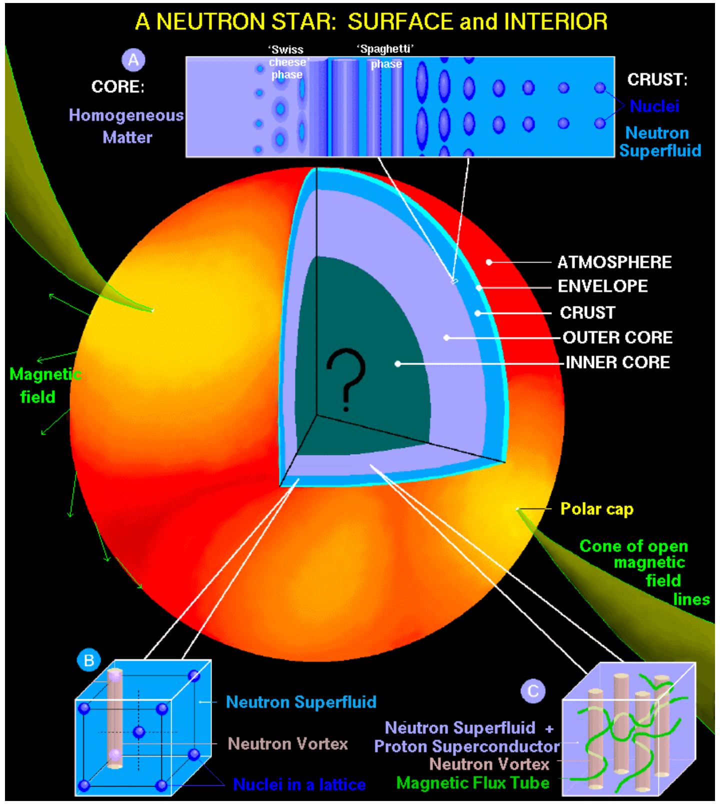

Danny Page (UNAM)

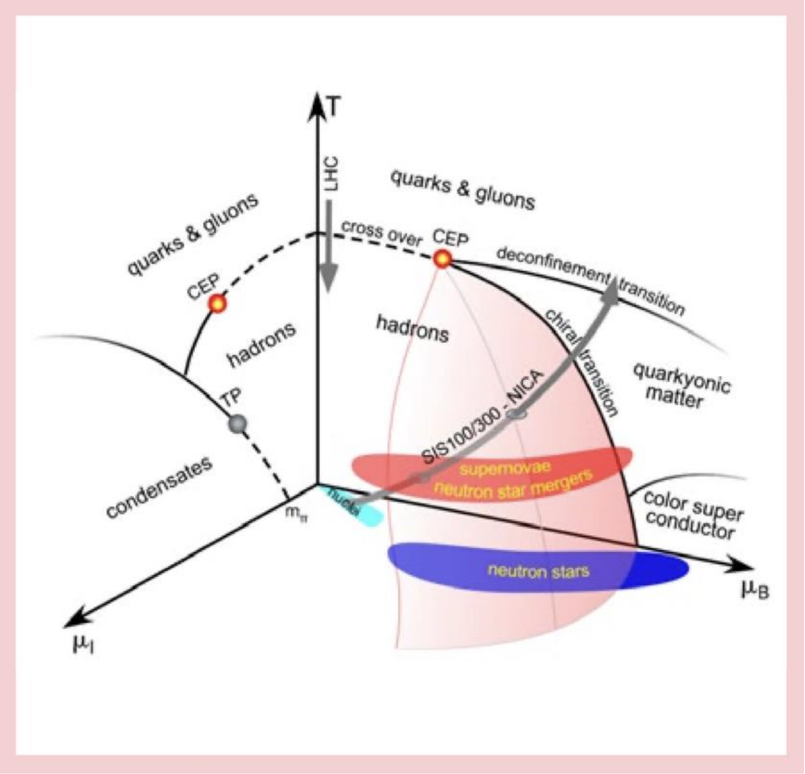

https://www.nupecc.org/lrp2016/Documents/lrp2017.pdf

NSs are great tools to study dense matter

Colliders: space vs terrestrial

PHYSICAL REVIEW D **107,** 043034 (2023)

Probing neutron-star matter in the lab: Similarities and differences between binary mergers and heavy-ion collisions

Elias R. Most,[1,2,3] Anton Motornenko,[4,5] Jan Steinheimer,[5] Veronica Dexheimer,[6] Matthias Hanauske,[4,5] Luciano Rezzolla,[4,5,7] and Horst Stoecker[4,5,8]

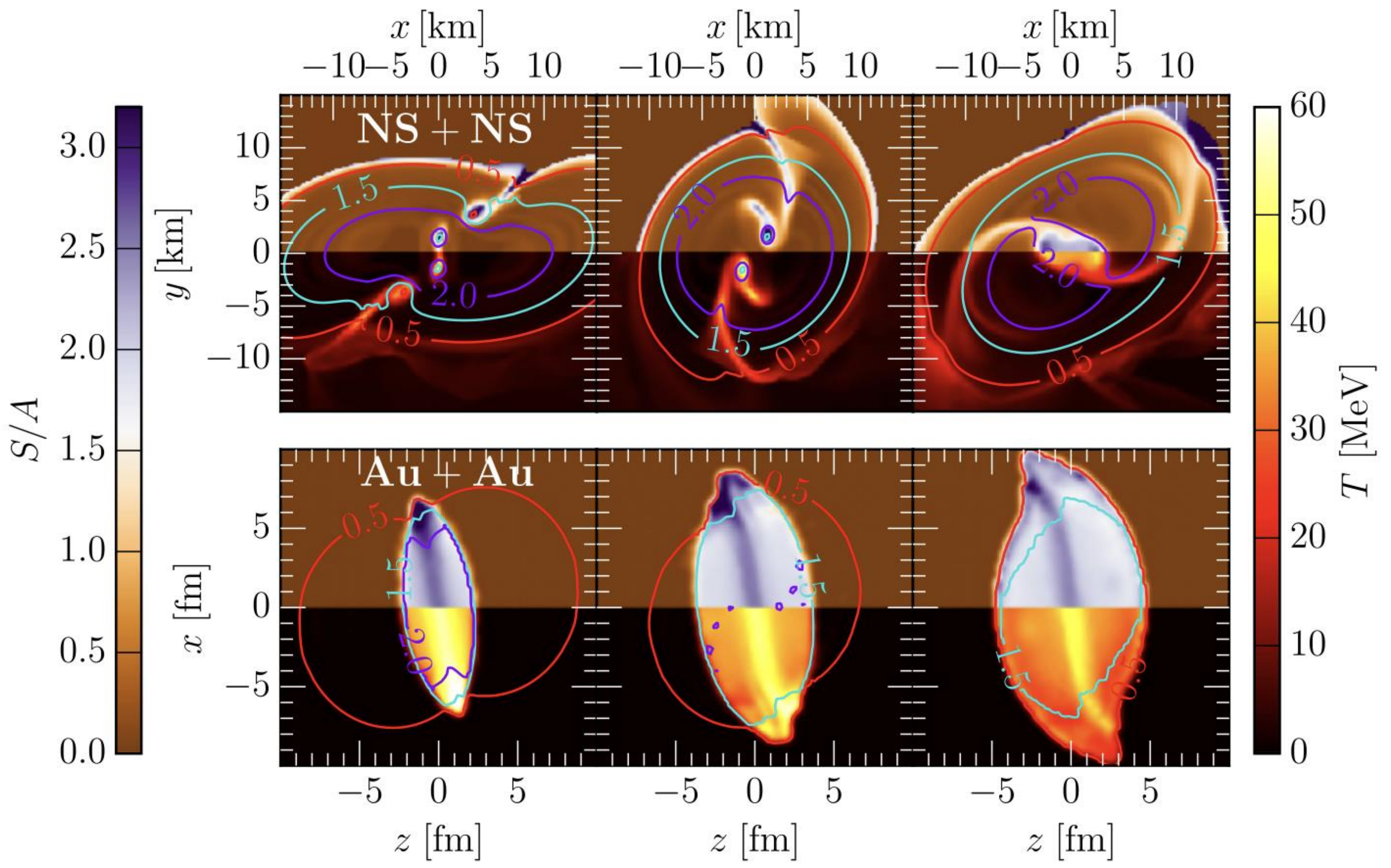

FIG. 2. Distributions of entropy per baryon S/A (upper color maps) and temperature T (lower color maps) for a BNSM (NS + NS) with total mass $M_{\rm tot} = 2.8 M_\odot$ (top panels) and a Au + Au HIC at $E_{\rm lab} = 450A\mathrm{MeV}$ (bottom panels). Colored lines mark density contours in units of $n_{\rm sat}$. The snapshots in different rows refer to $t = -2, 0, +3$ ms before and after merger for the BNSM, respectively, and to $t = -5, 0, +5,$ fm/c before and after the full overlap for the HIC.

Colliders: space vs terrestrial

PHYSICAL REVIEW D **107**, 043034 (2023)

Probing neutron-star matter in the lab: Similarities and differences between binary mergers and heavy-ion collisions

Elias R. Most,[1,2,3] Anton Motornenko,[4,5] Jan Steinheimer,[5] Veronica Dexheimer,[6] Matthias Hanauske,[4,5] Luciano Rezzolla,[4,5,7] and Horst Stoecker[4,5,8]

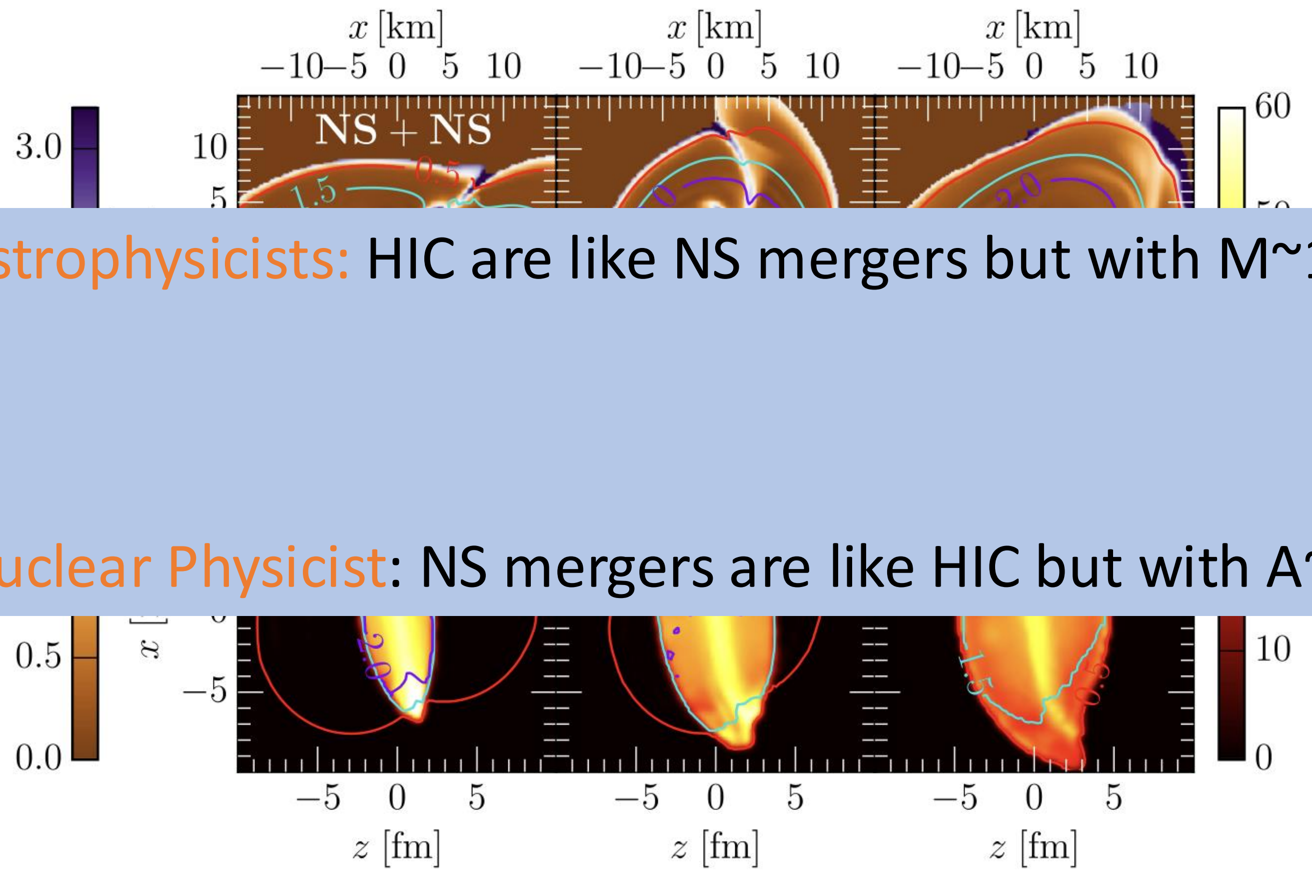

For Astrophysicists: HIC are like NS mergers but with M~10^{-22} g

For Nuclear Physicist: NS mergers are like HIC but with A~10^{57}

FIG. 2. Distributions of entropy per baryon S/A (upper color maps) and temperature T (lower color maps) for a BNSM (NS + NS) with total mass $M_{tot} = 2.8M_{\odot}$ (top panels) and a Au + Au HIC at $E_{lab} = 450A\text{MeV}$ (bottom panels). Colored lines mark density contours in units of n_{sat}. The snapshots in different rows refer to $t = -2, 0, +3$ ms before and after merger for the BNSM, respectively, and to $t = -5, 0, +5$, fm/c before and after the full overlap for the HIC.

Neutron star matter

- Atmosphere (~10 cm)
  - On top of the ocean
  - Mostly gas
- Ocean (1-100 m)
  - Iron (isolated NS)
  - H, He (accreting NS)
- Crust (1 km)
  - Outer crust (ionized atoms)
  - Neutron drip 4.3x10^{11} g.cm^{-3}
  - Inner crust
    - Nuclei are very neutron rich – clusters
    - Free neutrons may be superfluid
    - Pasta on the bottom (mantle)

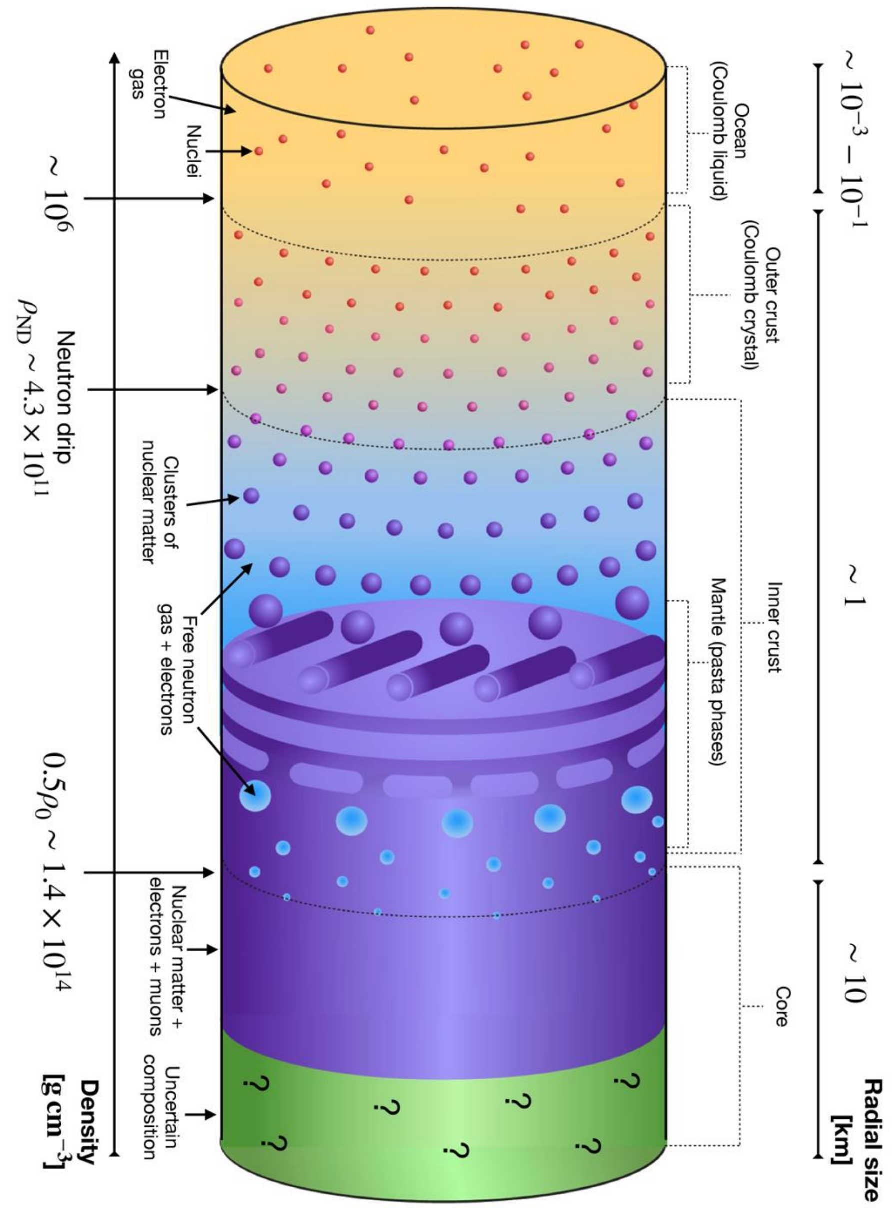

Ascenzi, S.; Graber, V.; Rea N.: Astroparticle Physics, 2024

Neutron star matter

- Core (~10 km)
  - Starts at about ½ of saturation density =2.8×10^{14} g.cm^{-3}
  - n,p,e in β-equilibrium (and charge neutrality)
  - $n_p \sim 1/8\, n_n$
  - Possible Bose-Einstein condensates (pion, kaon)
  - Quark-gluon plasma

  - Largely unknow matter but has a huge impact on neutron star properties

- Description of matter transfers to equation of state – combination of corresponding values of density, pressure and temperature (T -> 0 in most cases)

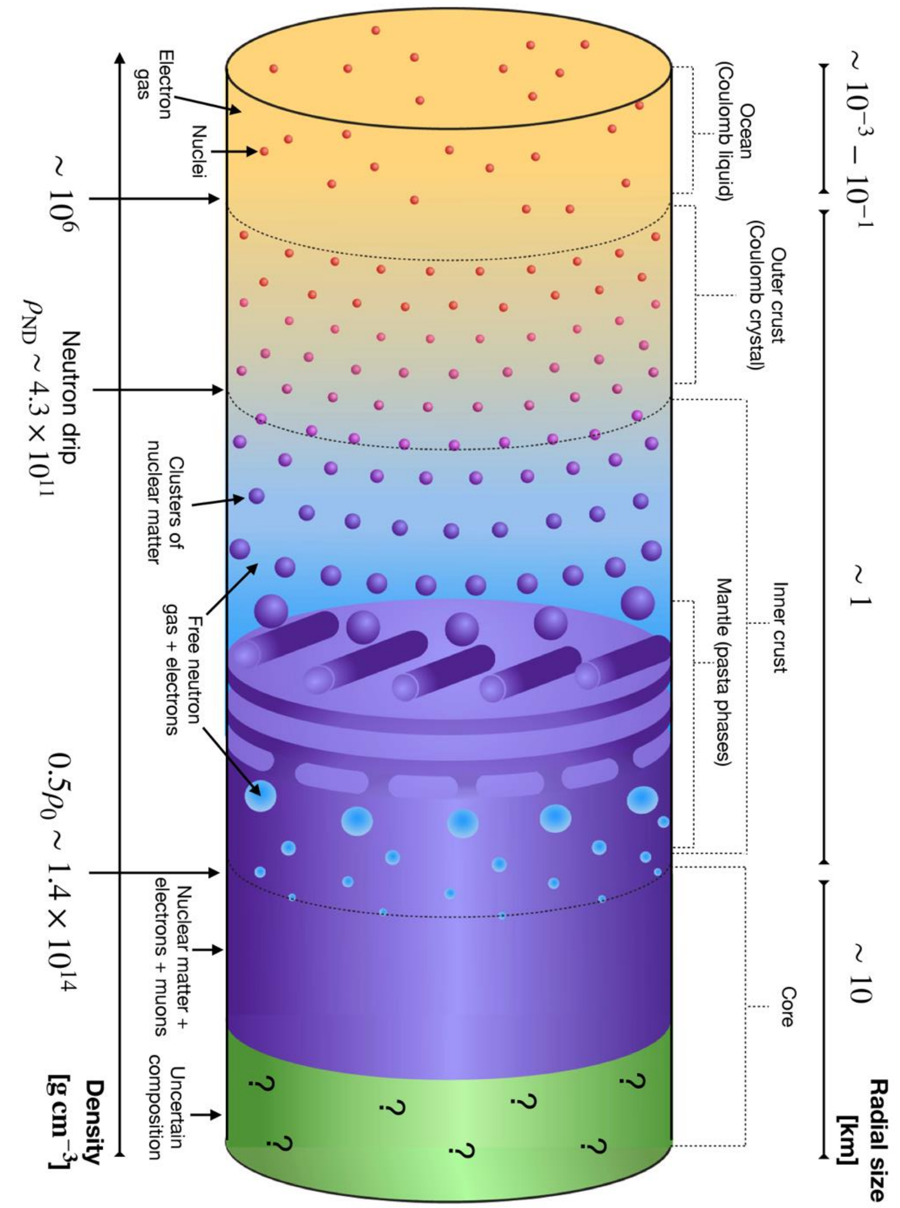

Ascenzi, S.; Graber, V.; Rea N.: Astroparticle Physics, 2024

Equation of state -> NS model

- From nuclear physics: Binding energy as a function of baryon density and composition
- NS equilibrium – charge neutrality + equilibrium (e.g. β) -> e(n)
- First law of thermodynamics -> $P=n^2\, \partial e/\partial n$
- Equation of state in the form P(e)

- Equation of hydrostatic equilibrium + conservation of mass

$$e^{2\Lambda} = \left(1 - \frac{2m_r}{r}\right)^{-1},$$

$$\frac{d\Phi}{dr} = -\frac{1}{\epsilon + p}\frac{dp}{dr},$$

$$\frac{dp}{dr} = -(\epsilon + p)\frac{m_r + 4\pi r^3 p}{r(r - 2m_r)},$$

$$\frac{dm_r}{dr} = 4\pi r^2 \epsilon.$$

Equation of state -> NS model

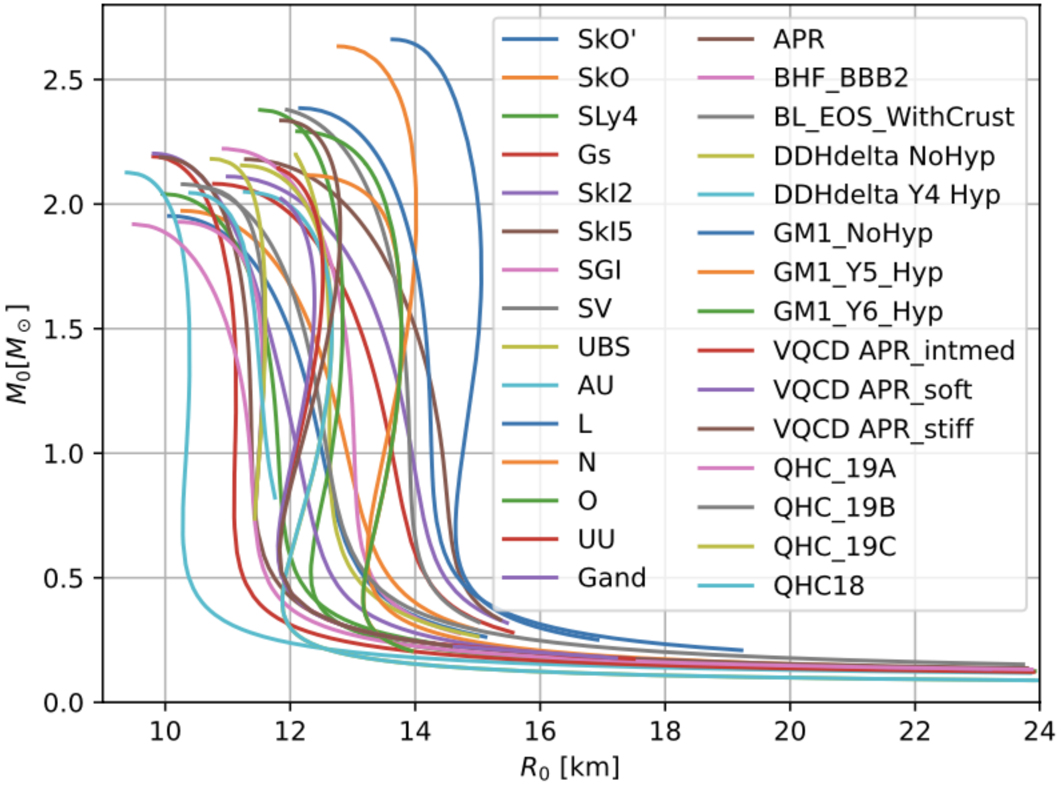

Equations of state taken from the compose database
(https://compose.obspm.fr)

[TOK_2015] S. Typel, M. Oertel, T. Klähn, Phys.Part.Nucl. 46, 633
[OHKT_2017] M. Oertel, M. Hempel, T. Klähn, S. Typel, Rev. Mod. Phys. 89, 015007
[TOK_2022] S. Typel, M. Oertel, T. Klähn et al, arxiv:2203.03209

There are dozens of models with hundreds of parametrizations

Perturbed stars – rotation/tides

- Hartle Thorne approach (slow rotation)

$$
\begin{aligned}
\mathrm{d}s^2 = & -\mathrm{e}^{2\nu}[1 + 2h_0(r) + 2h_2(r)P_2]\mathrm{d}t^2 \\
& + \mathrm{e}^{2\lambda}\left\{1 + \frac{\mathrm{e}^{2\lambda}}{r}[2m_0(r) + 2m_2(r)P_2]\right\}\mathrm{d}r^2 \\
& + r^2[1 + 2k_2(r)P_2]\left\{\mathrm{d}\theta^2 + [\mathrm{d}\phi - \omega(r)\mathrm{d}t]^2\sin^2\theta\right\},
\end{aligned}
$$

- Differential equations for perturbation functions are obtained from Einstein equations
- We match exterior and interior solution

-> *M*, *J*, *Q*

Dimensionless, frequency ind. quantities

- Nonrotating star M_0 R_0
- Rotating stars M, Q, J, f
- Dimensionless, frequency independent quantities

  $R_0/M_0,\ QM_0/J^2,\ I/M^3\ (I=J/f)$

Tidal deformability and Love numbers

- Tidal deformability $\Lambda = 2/3\ k_2\ (M/R)^5$
- Love number $(l=2)\ k_2$

Rotating stars

- Moment of inertia and quadrupole moment

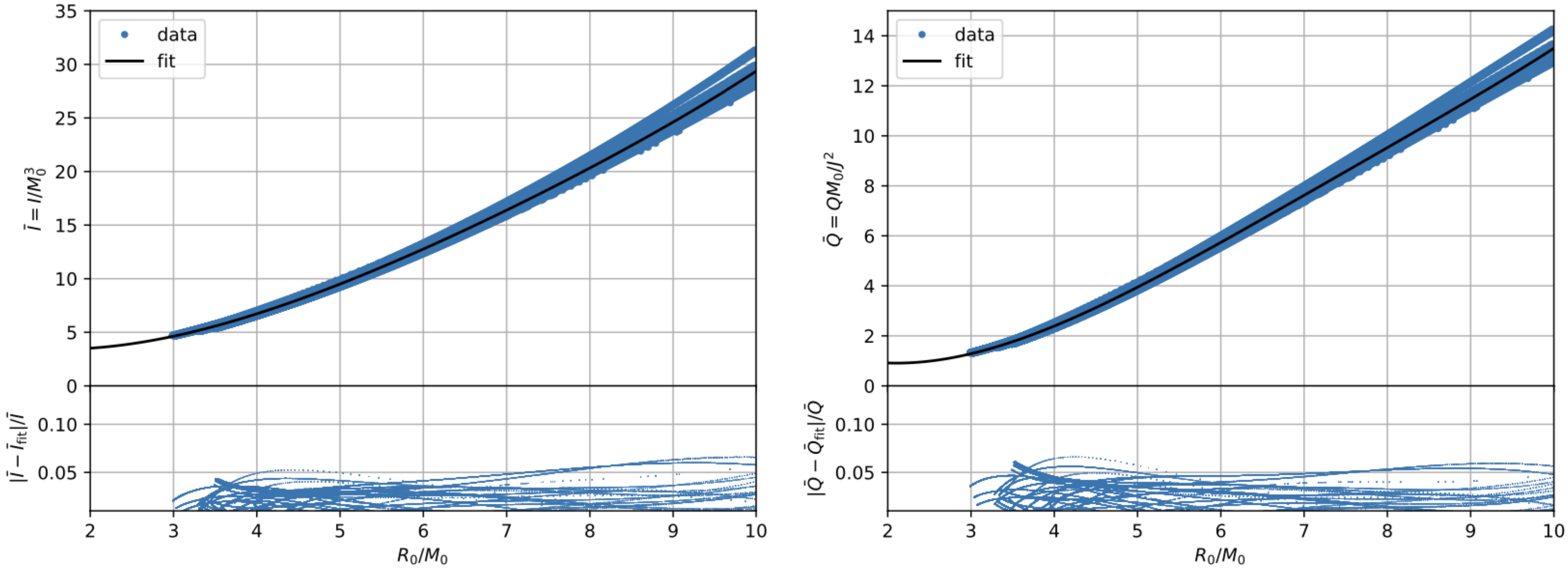

Rotating stars

- Change in shape of the star and total gravitational mass

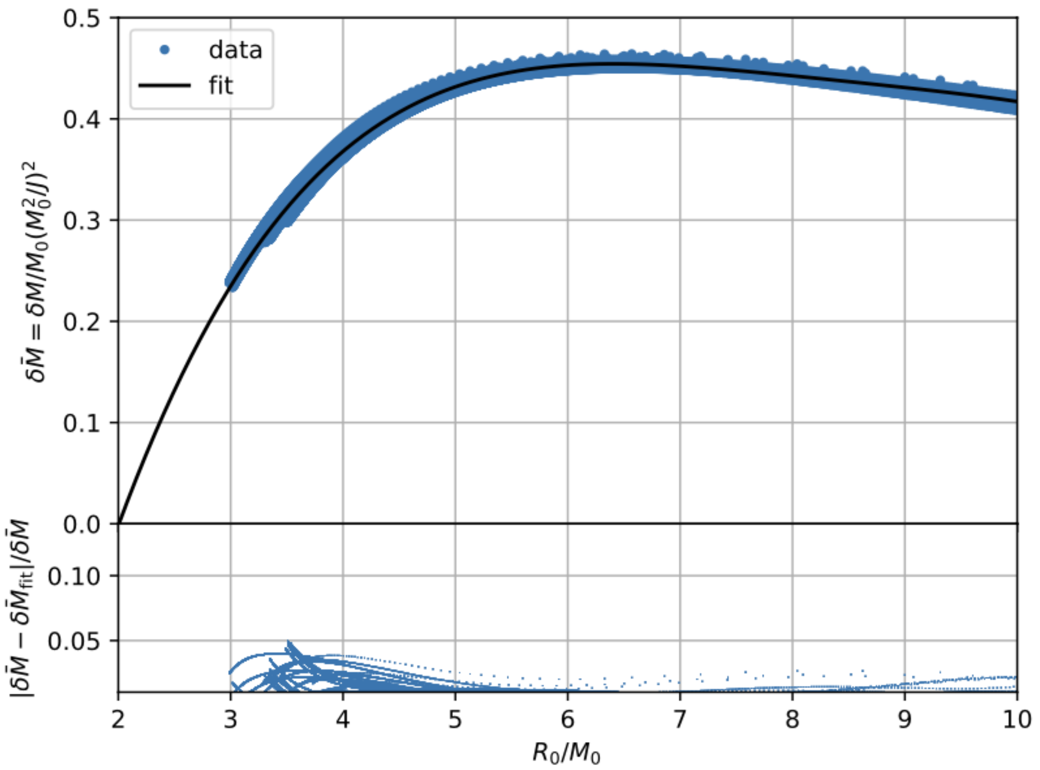

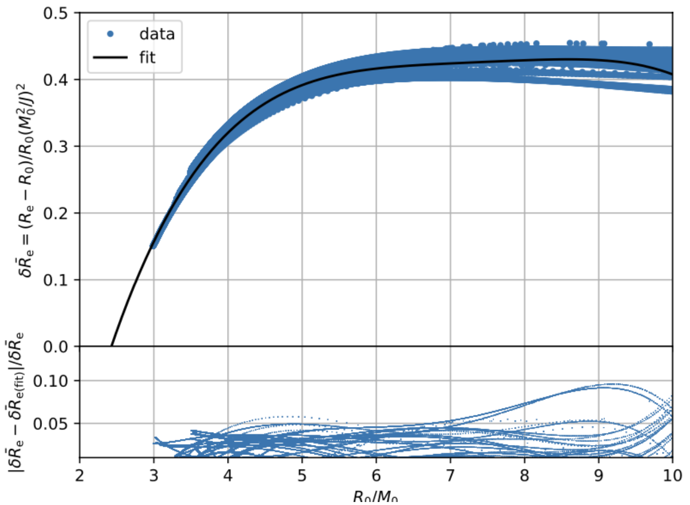

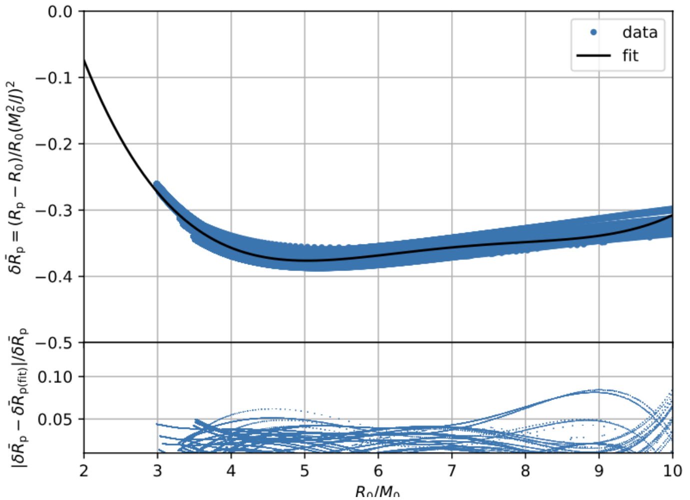

Love numbers and tidal deformability

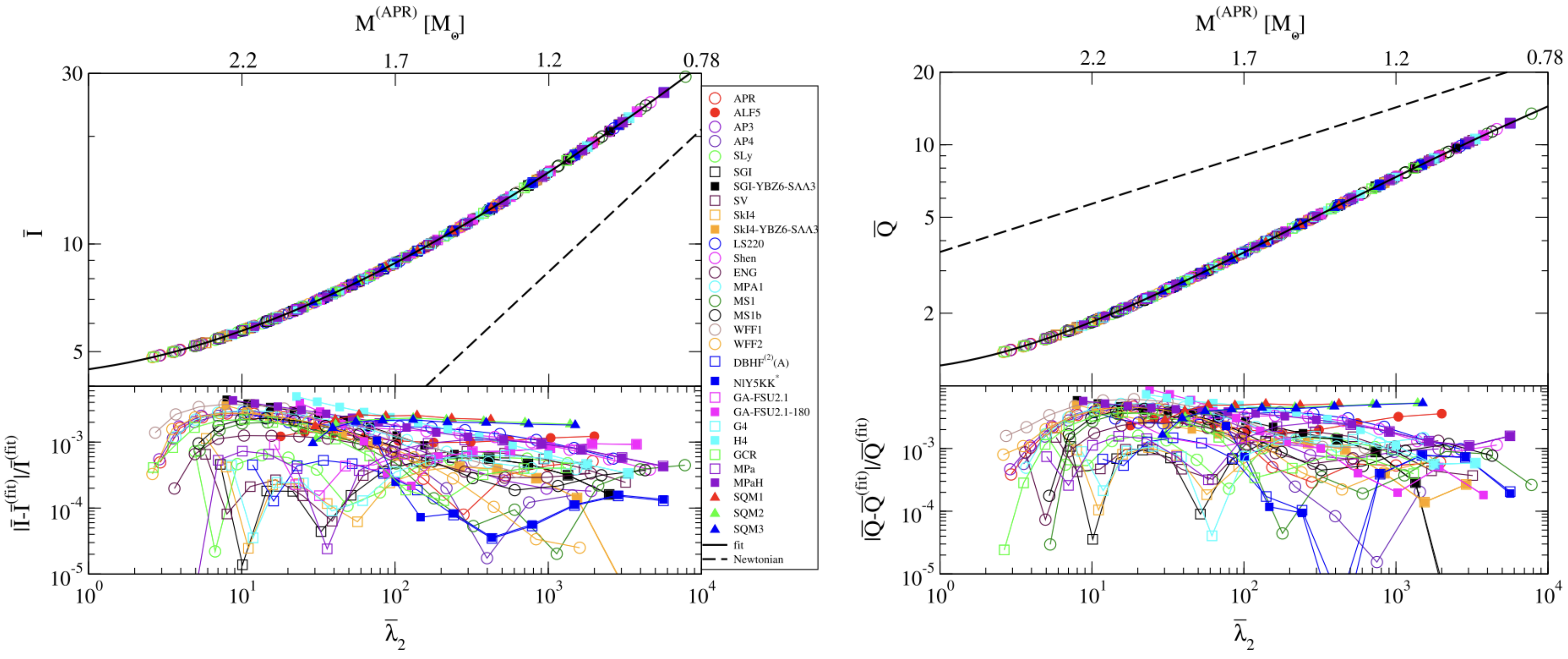

Fig. 3. (Top) The universal I–Love (left) and Q–Love (right) relations for slowly-rotating neutron stars and quark stars of $1M_\odot < M < M^{(\max)}$ with various equations of state. A single parameter along the curve is the stellar mass or compactness, which increases to the left of the plots. The solid curves show the fit in Eq. (15). The top axis shows the corresponding stellar mass of an isolated, non-rotating configuration with the APR equation of state. (Bottom) Absolute fractional difference from the fit, while the dashed lines show the analytic Newtonian relations in Eq. (11) with $n = 0$. Observe that the relations are equation-of-state insensitive to $\mathcal{O}(1\%)$.

Yagi & Yunes, 2017, Phys. Rep.

Love numbers and tidal deformability

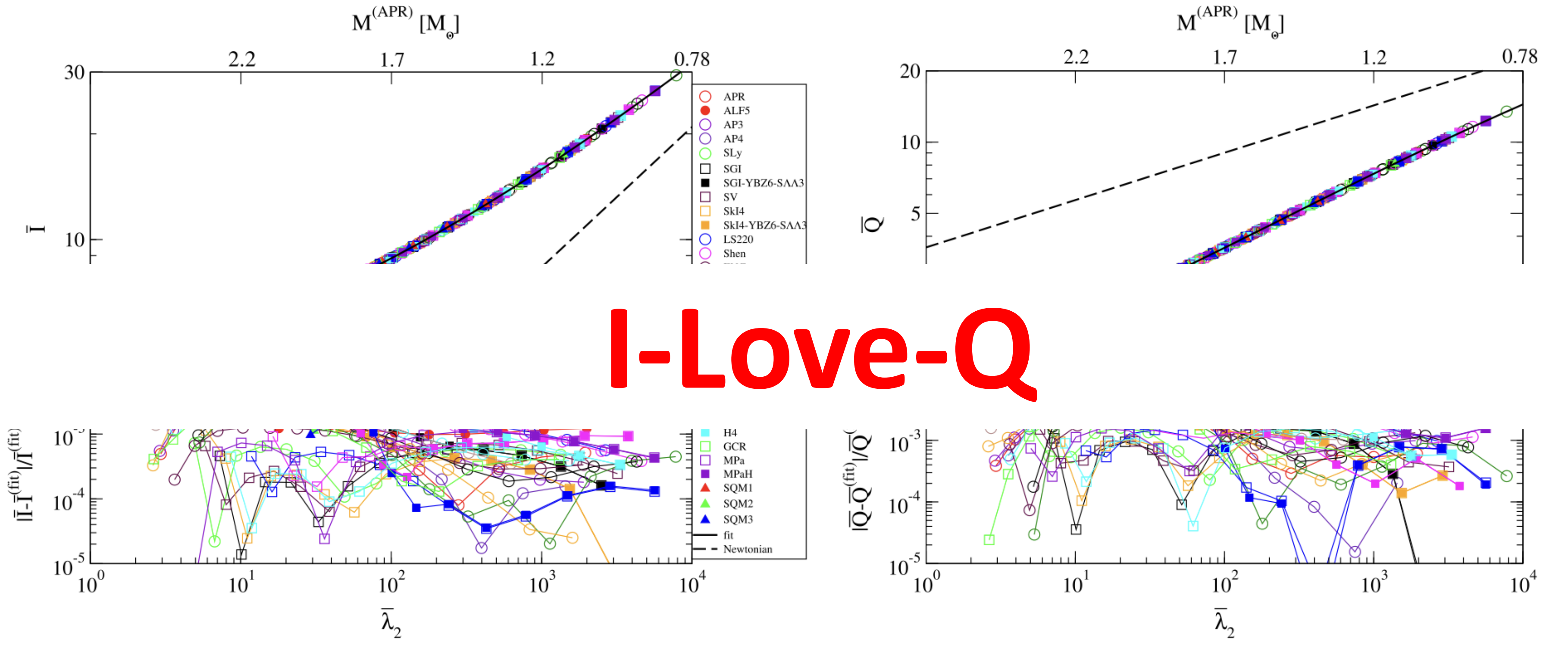

Fig. 3. (Top) The universal I–Love (left) and Q–Love (right) relations for slowly-rotating neutron stars and quark stars of $1M_\odot < M < M^{(\max)}$ with various equations of state. A single parameter along the curve is the stellar mass or compactness, which increases to the left of the plots. The solid curves show the fit in Eq. (15). The top axis shows the corresponding stellar mass of an isolated, non-rotating configuration with the APR equation of state. (Bottom) Absolute fractional difference from the fit, while the dashed lines show the analytic Newtonian relations in Eq. (11) with $n = 0$. Observe that the relations are equation-of-state insensitive to $\mathcal{O}(1\%)$.

Yagi & Yunes, 2017, Phys. Rep.

Can we find a difference between hybrid and nuclear EoS?

- Separate EoS from compose to two distinct classes
  - Nucleonic
  - Hybrid

- Calculate M-R and tidal deformability

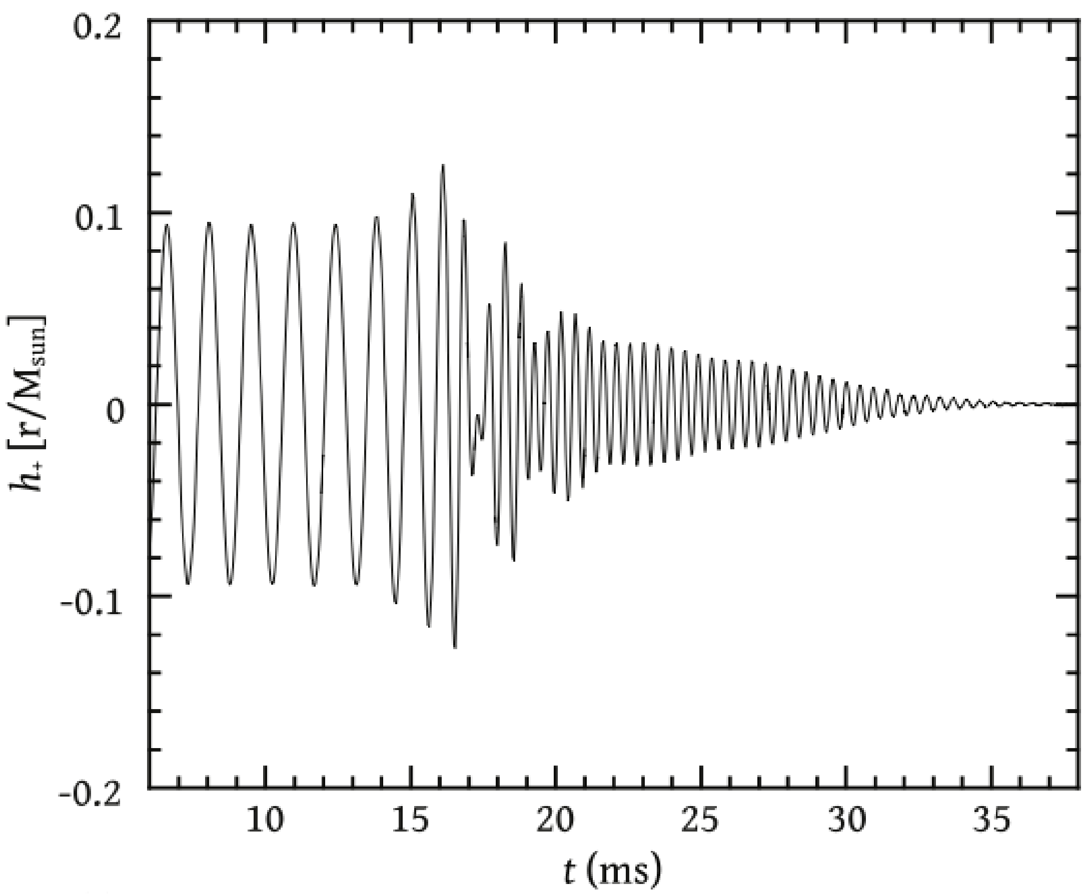

Stergioulas et al 2011, MNRAS

Equation of state -> NS model

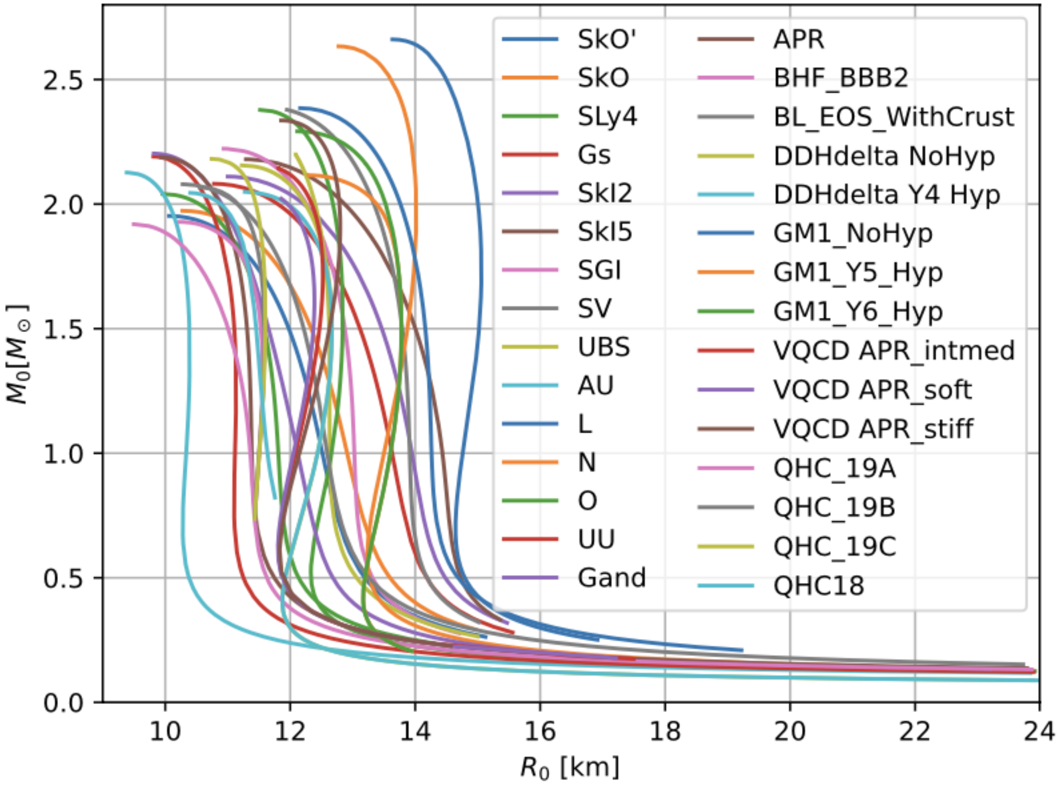

Equations of state taken from the compose database (https://compose.obspm.fr)

[TOK_2015] S. Typel, M. Oertel, T. Klähn, Phys.Part.Nucl. 46, 633
[OHKT_2017] M. Oertel, M. Hempel, T. Klähn, S. Typel, Rev. Mod. Phys. 89, 015007
[TOK_2022] S. Typel, M. Oertel, T. Klähn et al, arxiv:2203.03209

There are dozens of models with hundreds of parametrizations

Equ

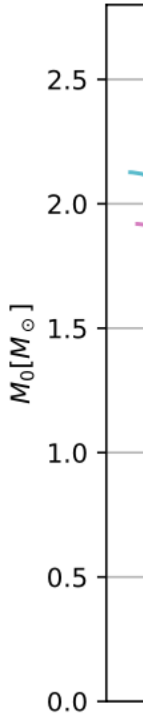

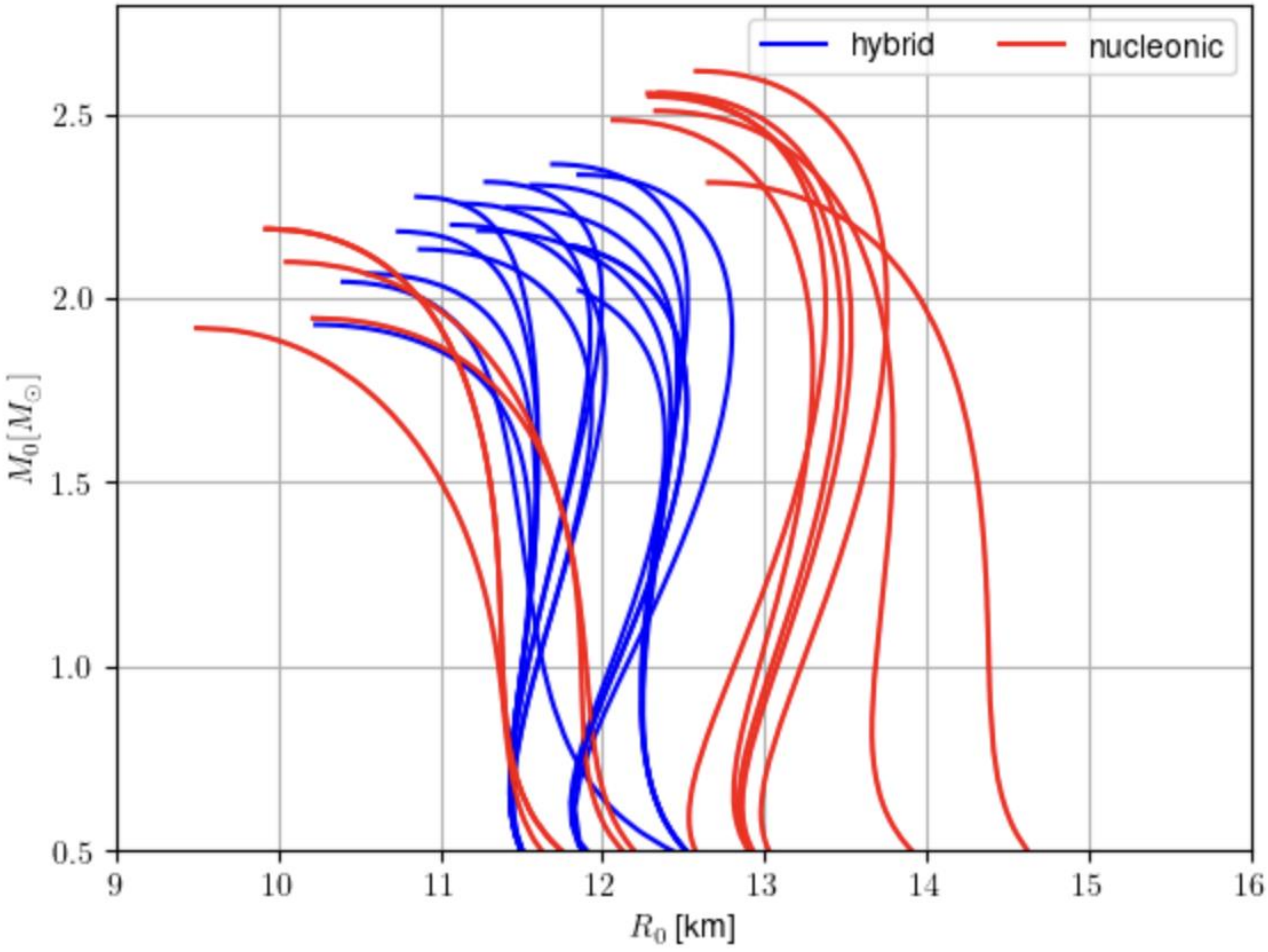

he compose

pm.fr)

el, T. Klähn,

empel, T. Klähn,
15007
el, T. Klähn et al,

hundreds of

Tidal deformability and Love numbers

- Tidal deformability $\Lambda = 2/3\ k_2\ (M/R)^5$
- Love number *(l=2)* k_2

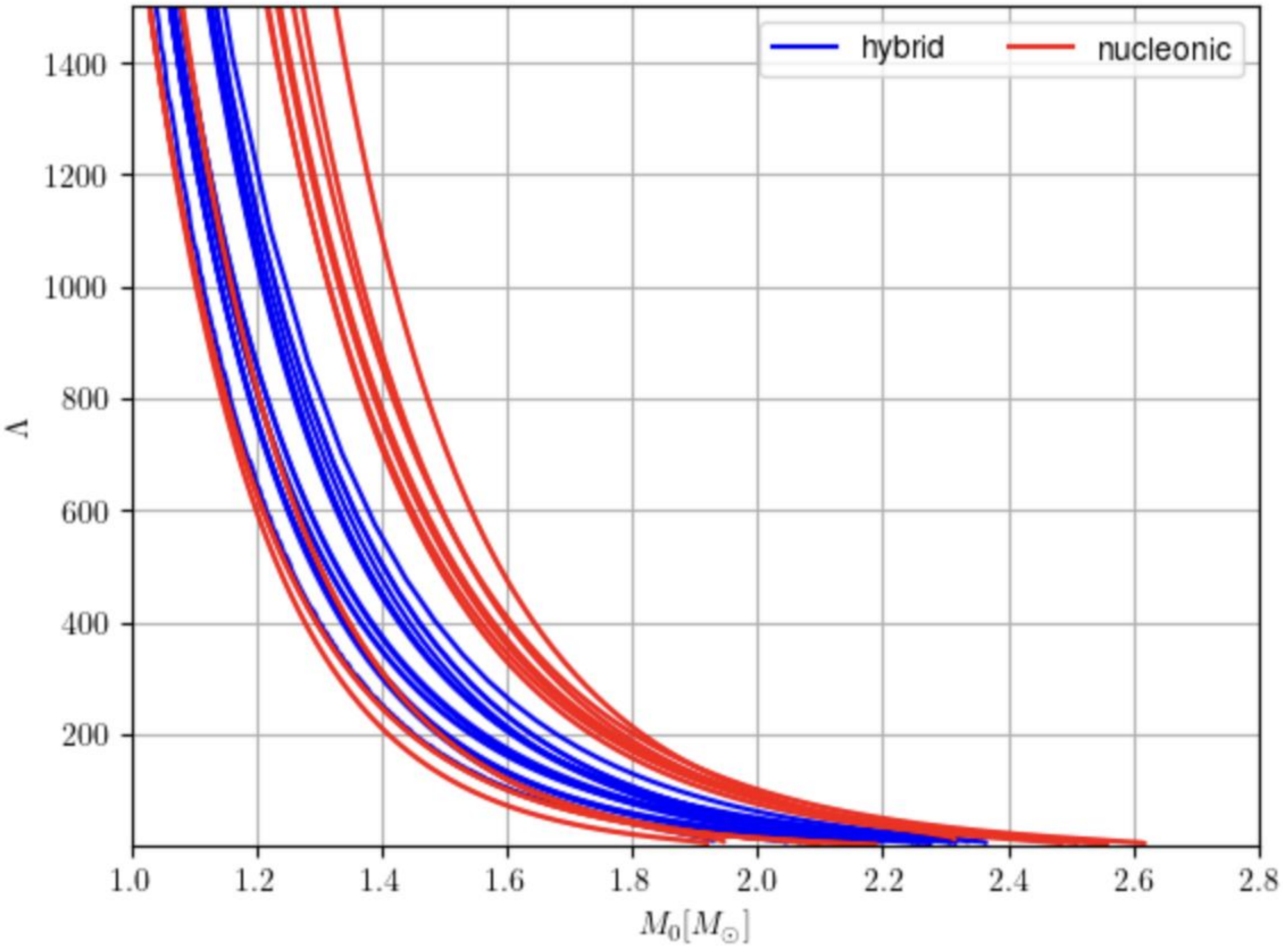

It is difficult to distinguished from tidal deformability

- Another approach
  - Assume we know the nucleonic EoS
  - Can we see the deviation if the quark core is present

- Master project of Ondřej Chlopčík
  - Take one nucleonic EoS and assume there is quark core present
  - We took it to rather extreme case, where the hybrid stars can have rather small maximum mass

Ondřej's results

- NRAPR EoS
- Bag model for quarks

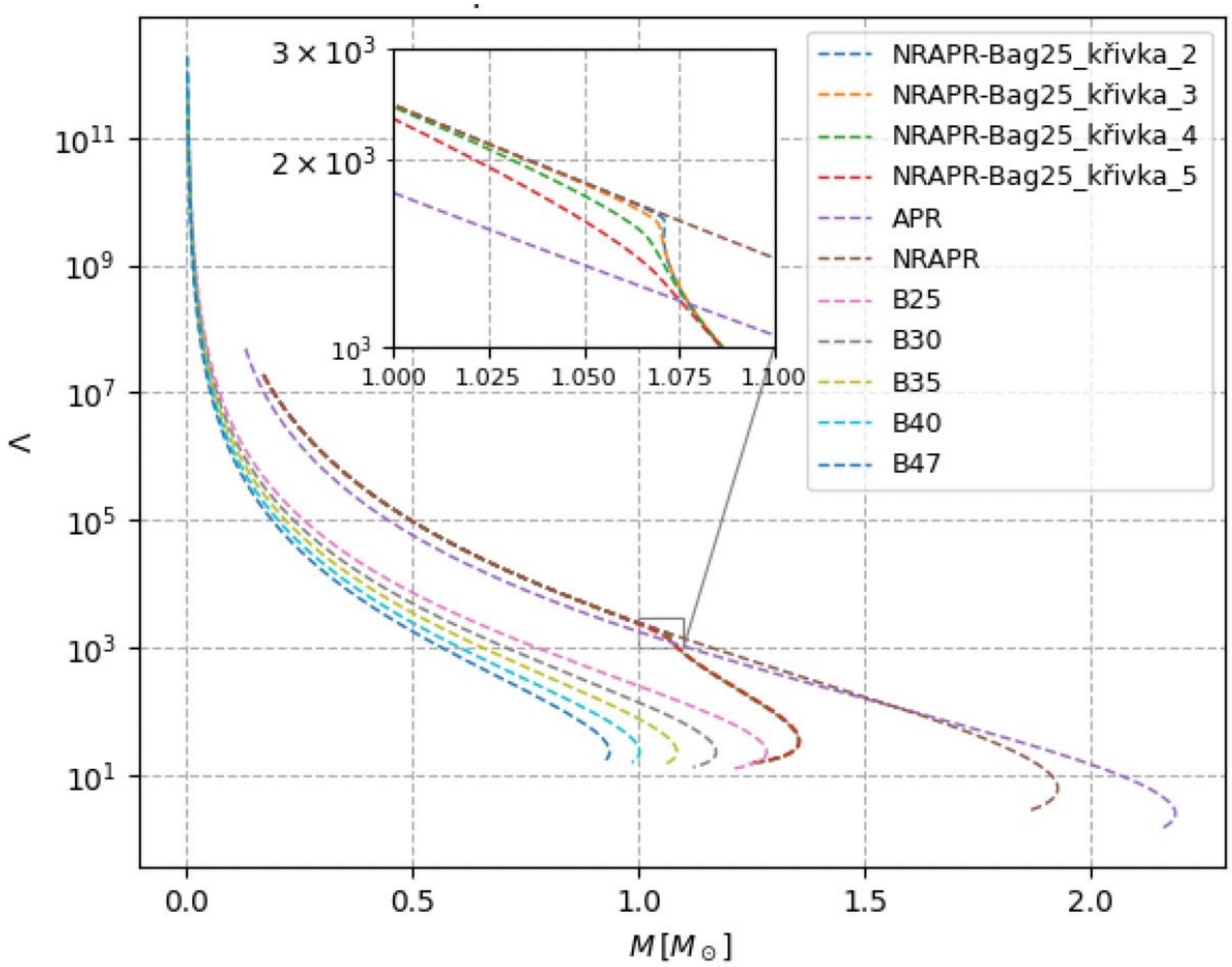

Conclusions and future plans

- NS mergers can be used to constrain equation of state of dense matter
- For phase-transitions best diagnostic tool is post-merger evolution
- Two main approaches are used
  - Universal relations

    + directly connected with equations of state, computational extremely cheap

    - may be wrong if used in parts of M-R plane that are not cowered by EoS
  - Analytical approximation to EoS

    + constraints on parameters can be combined for more sources

    - computationally more expensive, may be too strict for EoS

- We will combine these two – use tabular EoS for the outer parts and analytical representation for the quark matter core
- Use machine learning techniques for estimations of EoS parameters

GW170817

- First merger of 2 NS
- Multi-messenger observations
- Measurements of Neutron Star Radii and EoS (1 year later) from tidal deformability
- Other constraints from post-merger evolutior

Selected for a Viewpoint in *Physics*

PRL **119,** 161101 (2017) PHYSICAL REVIEW LETTERS week ending 20 OCTOBER 2017

GW170817: Observation of Gravitational Waves from a Binary Neutron Star Inspiral

B. P. Abbott *et al.**

(LIGO Scientific Collaboration and Virgo Collaboration)

(Received 26 September 2017; revised manuscript received 2 October 2017; published 16 October 2017)

The Astrophysical Journal Letters, 848:L12 (59pp), 2017 October 20 https://doi.org/10.3847/2041-8213/aa91c9

© 2017. The American Astronomical Society. All rights reserved.

OPEN ACCESS

CrossMark

Multi-messenger Observations of a Binary Neutron Star Merger*

LIGO Scientific Collaboration and Virgo Collaboration, Fermi GBM, INTEGRAL, IceCube Collaboration, AstroSat Cadmium Zinc Telluride Imager Team, IPN Collaboration, The Insight-HXMT Collaboration, ANTARES Collaboration, The Swift Collaboration, AGILE Team, The 1M2H Team, The Dark Energy Camera GW-EM Collaboration and the DES Collaboration, The DLT40 Collaboration, GRAWITA: GRAvitational Wave Inaf TeAm, The Fermi Large Area Telescope Collaboration, ATCA: Australia Telescope Compact Array, ASKAP: Australian SKA Pathfinder, Las Cumbres Observatory Group, OzGrav, DWF (Deeper, Wider, Faster Program), AST3, and CAASTRO Collaborations, The VINROUGE Collaboration, MASTER Collaboration, J-GEM, GROWTH, JAGWAR, Caltech-NRAO, TTU-NRAO, and NuSTAR Collaborations, Pan-STARRS, The MAXI Team, TZAC Consortium, KU Collaboration, Nordic Optical Telescope, ePESSTO, GROND, Texas Tech University, SALT Group, TOROS: Transient Robotic Observatory of the South Collaboration, The BOOTES Collaboration, MWA: Murchison Widefield Array, The CALET Collaboration, IKI-GW Follow-up Collaboration, H.E.S.S. Collaboration, LOFAR Collaboration, LWA: Long Wavelength Array, HAWC Collaboration, The Pierre Auger Collaboration, ALMA Collaboration, Euro VLBI Team, Pi of the Sky Collaboration, The Chandra Team at McGill University, DFN: Desert Fireball Network, ATLAS, High Time Resolution Universe Survey, RIMAS and RATIR, and SKA South Africa/MeerKAT

(See the end matter for the full list of authors.)

Received 2017 October 3; revised 2017 October 6; accepted 2017 October 6; published 2017 October 16

Abstract

GW170817: Measurements of Neutron Star Radii and Equation of State

B. P. Abbott *et al.**

(The LIGO Scientific Collaboration and the Virgo Collaboration)

(Received 5 June 2018; revised manuscript received 25 July 2018; published 15 October 2018)

GW170817 Mass and Radius Constraints

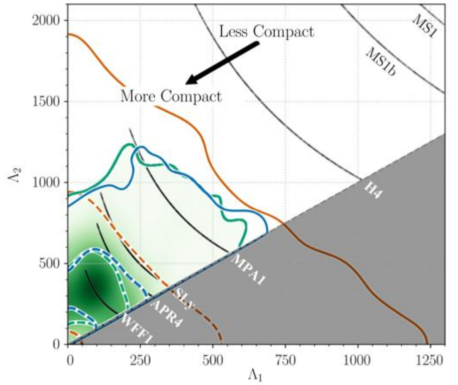

FIG. 1. Marginalized posterior for the tidal deformabilities of the two binary components of GW170817. The green shading shows the posterior obtained using the $\Lambda_a(\Lambda_s, q)$ EOS-insensitive relation to impose a common EOS for the two bodies, while the green, blue, and orange lines denote 50% (dashed) and 90% (solid) credible levels for the posteriors obtained using EOS-insensitive relations, a parametrized EOS without a maximum mass requirement, and independent EOSs (taken from [52]), respectively. The gray shading corresponds to the unphysical region $\Lambda_2 < \Lambda_1$ while the seven black scatter regions give the tidal parameters predicted by characteristic EOS models for this event [113,115,121–125].

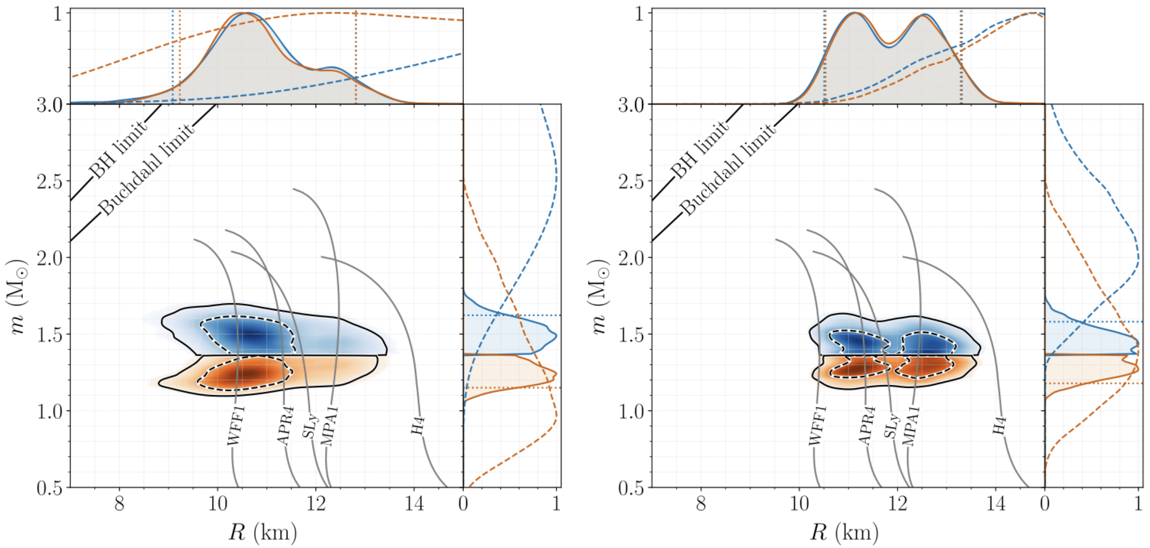

FIG. 3. Marginalized posterior for the mass m and areal radius R of each binary component using EOS-insensitive relations (left panel) and a parametrized EOS where we impose a lower limit on the maximum mass of 1.97 $M_\odot$ (right panel). The top blue (bottom orange) posterior corresponds to the heavier (lighter) NS. Example mass-radius curves for selected EOSs are overplotted in gray. The lines in the top left denote the Schwarzschild BH ($R = 2m$) and Buchdahl ($R = 9m/4$) limits. In the one-dimensional plots, solid lines are used for the posteriors, while dashed lines are used for the corresponding parameter priors. Dotted vertical lines are used for the bounds of the 90% credible intervals.

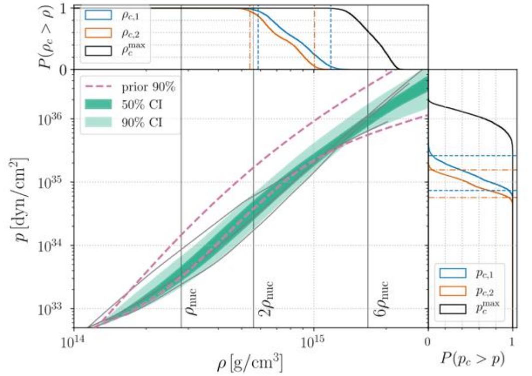

FIG. 2. Marginalized posterior (green bands) and prior (purple dashed) for the pressure p as a function of the rest-mass density ρ of the NS interior using the spectral EOS parametrization and imposing a lower limit on the maximum NS mass supported by the EOS of 1.97 $M_\odot$. The dark (light) shaded region corresponds to the 50% (90%) posterior credible level and the purple dashed lines show the 90% prior credible interval. Vertical lines correspond to once, twice, and six times the nuclear saturation density. Overplotted in gray are representative EOS models [121,122,124], using data taken from [19]; from top to bottom at $2\rho_{nuc}$ we show H4, APR4, and WFF1. The corner plots show cumulative posteriors of central densities ρ_c (top) and central pressures p_c (right) for the two NSs (blue and orange), as well as for the heaviest NS that the EOS supports (black). The 90% credible intervals for ρ_c and p_c are denoted by vertical and horizontal lines respectively for the heavier (blue dashed) and lighter (orange dot-dashed) NS.

GW170817: Measurements of Neutron Star Radii and Equation of State

B. P. Abbott *et al.**
(The LIGO Scientific Collaboration and the Virgo Collaboration)

(Received 5 June 2018; revised manuscript received 25 July 2018; published 15 October 2018)

How to constrain EoS from post-merger

PHYSICAL REVIEW LETTERS **122,** 061101 (2019)

Editors' Suggestion

Signatures of Quark-Hadron Phase Transitions in General-Relativistic Neutron-Star Mergers

Elias R. Most,[1] L. Jens Papenfort,[1] Veronica Dexheimer,[2] Matthias Hanauske,[1,3] Stefan Schramm,[1,3] Horst Stöcker,[1,3,4] and Luciano Rezzolla[1,3]

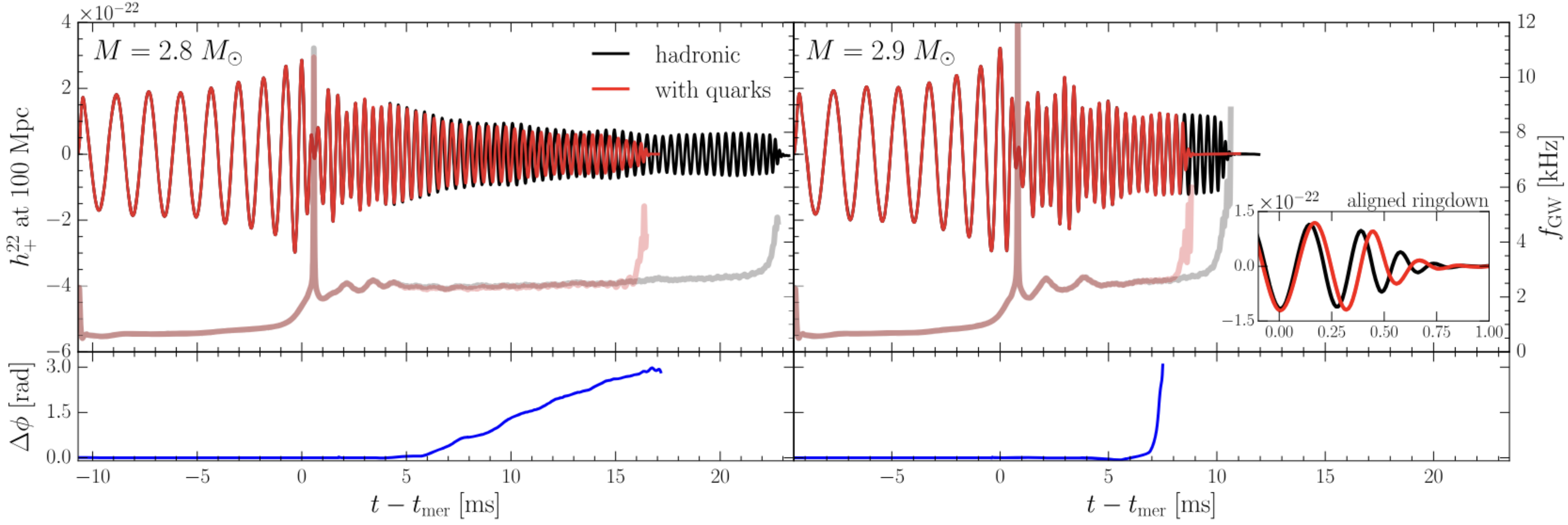

FIG. 4. Properties of the GW emission for the low- (left-hand panels) and high-mass binaries (right-hand panels). The top panels report the strain h_+^{22} for the two EOSs, together with the instantaneous GW frequency $f_{\rm GW}$ (semitransparent lines). The bottom panels show the phase difference $\Delta\Phi$ between the two signals. The inset in the top right-hand panel highlights the differences in the ringdown.

How to constrain EoS from post-merger

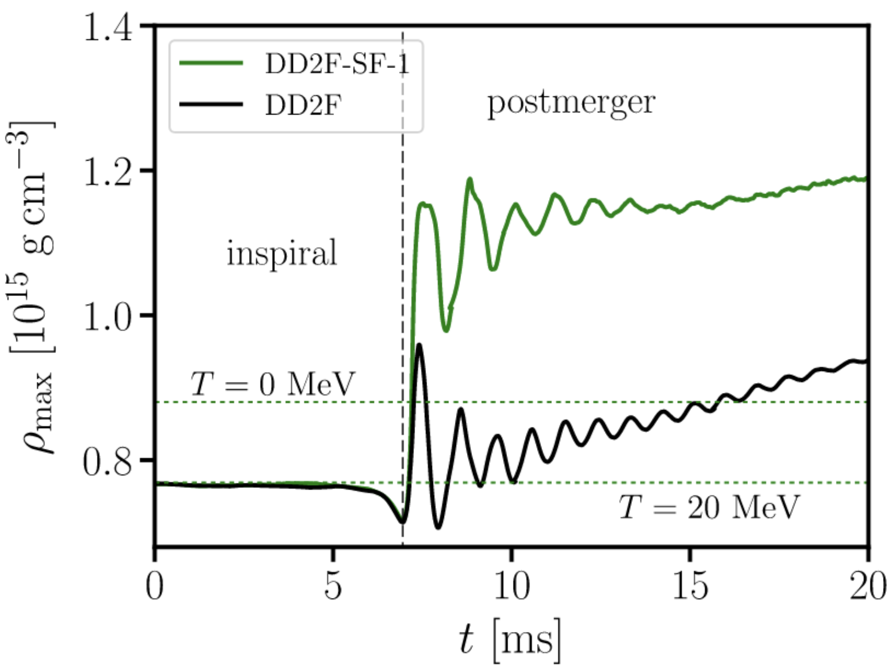

FIG. 1. Evolution of the maximum rest-mass density comparing DD2F-SF-1 (green line) and DD2F (black line) for $1.35\ M_\odot - 1.35\ M_\odot$ mergers (solid curves). Horizontal dotted green lines mark the onset density ρ_{onset} of the phase transition for DD2F-SF-1 at $T = 0$ and at 20 MeV.

PHYSICAL REVIEW LETTERS **122,** 061102 (2019)

Editors' Suggestion

Identifying a First-Order Phase Transition in Neutron-Star Mergers through Gravitational Waves

Andreas Bauswein,[1] Niels-Uwe F. Bastian,[2] David B. Blaschke,[2,3] Katerina Chatziioannou,[4,7] James A. Clark,[5] Tobias Fischer,[2] and Micaela Oertel[6]

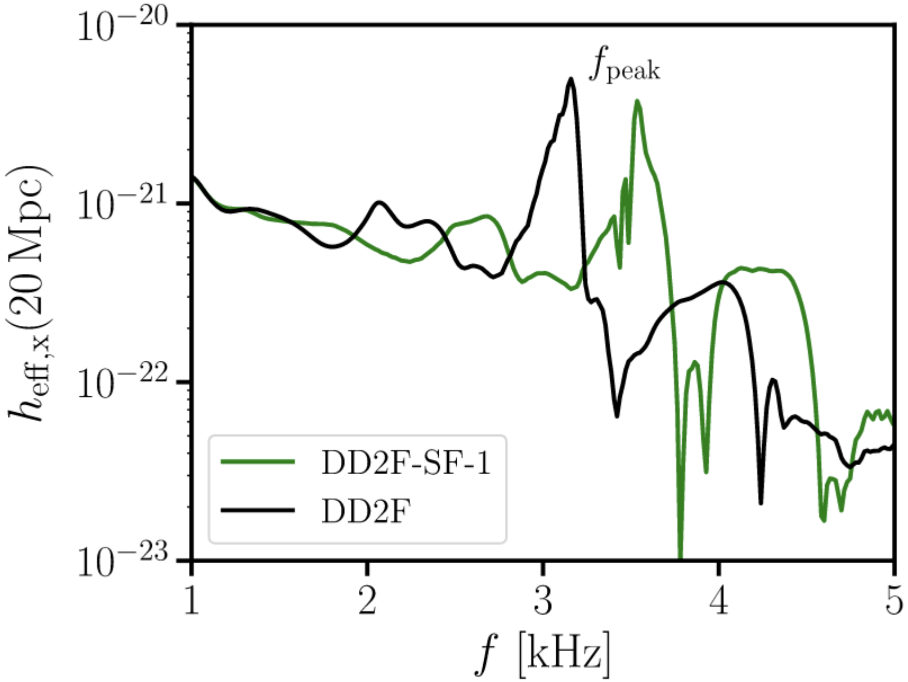

FIG. 2. GW spectrum of the cross polarization at a distance of 20 Mpc along the polar axis comparing the DD2F-SF-1 EOS (green curve) and the DD2F EOS (black curve).